PILOT STUDY OF BLAST PERFORMANCE OF REINFORCED CONCRETE RESERVOIR WALLS

Jin Fan, M.A.Sc. in Civil Engineering, Department of Civil Engineering, University of Ottawa, Ottawa, ON, Canada, Email: jin058.fan@gmail.com
Dan Palermo, Associate Professor, Department of Civil Engineering, Lassonde School of Engineering, York University, Toronto, ON, Canada, Email: dan.palermo@lassonde.yorku.ca
Ioan Nistor, Associate Professor, Department of Civil Engineering, University of Ottawa, Ottawa, ON, Canada, Email: inistor@uottawa.ca

Abstract: Reinforced concrete reservoir tanks are commonly used for water and wastewater storage and treatment. Given their function and importance to society, intentional or accidental blast loading of such structures could result in serious implications. This paper presents experimental results of two, scaled reservoir walls based on a prototype reservoir tank with the capacity to retain 10,000 m^3 of water. The reservoir tank walls were scaled according to the geometry and loading capacity of the shock tube housed in the Structures Laboratory at the University of Ottawa. The reservoir walls were designed and analyzed following the design method prescribed in Circular Concrete Tanks without Prestressing, published by the Portland Cement Association (PCA). The PCA method is largely based on the American Concrete Institute (ACI) 350 specifications. The experimental program was conducted with a shock tube that has the capability to impose short duration loads with characteristics similar to those of live explosives. The reservoir walls were subjected to incrementally increasing blast pressures to cover both elastic and inelastic response. The results presented in this paper include reflected pressures and impulses imposed on the walls, displacement- and reinforcement strain-time histories, cracking patters, and damage.

1 INTRODUCTION

1.1 General Background

Reinforced concrete reservoir tanks are commonly used for water and wastewater storage. They are considered critical infrastructure and are accessible to the public, therefore vulnerable to accidental or intentional attacks such as blast loading.

When a blast event occurs, the exterior elements of a structure are subjected to direct pressures from the blast. Explosives result in significant overpressures of a very short duration. Therefore, explosions lead to highly dynamic loadings on the structure. The overpressures, as a result of the shock wave, will propagate through the atmosphere and arrive at the target structure. The fragments generated by the explosion and the shock loads produced by the energy of the detonation can cause damage to structures. The Single-Degree-Of-Freedom (SDOF) method has been widely used to predict the dynamic flexural response of concrete structures and in the design of protective structures subjected to blast loading. The widely accepted procedure to assess structural damage is through Pressure-Impulse (P-I) interaction diagrams which can be obtained from SDOF analysis or blast testing.

Research related to this study has focused on the dynamic response of Reinforced Concrete (RC) walls/slabs subjected to blast loading, including analytical, numerical and experimental studies (Tai et al. 2011; Zhou and Hao 2008; Magnusson 2007; Razaqpur et al. 2007; Xu and Lu 2006; Quan 2005; Durunovic 1998; Toutlemonde et al. 1995). Other studies on the dynamic response of RC structures subjected to blast loading have concentrated on the equivalent SDOF method. These studies have illustrated that the level of damage experienced by structural members as a result of blast loading is estimated by Pressure-Impulse (P-I) diagrams (Shi et al. 2010; El-Dakhakhni et al. 2010; Morison 2006; Lu et al. 2005; Li and Meng 2002). Research, however, that has specifically investigated reservoir walls is lacking.

1.2 Research Significance

Reservoirs are lifeline structures that play a vital role in the economy of a country. If reservoirs are targeted, the resulting damage can be catastrophic, rendering the stored water unusable or destroying the water supply infrastructure. Furthermore, damage resulting from terrorist attacks on reservoirs would cause ripple effects leading to the disruption of the functions of society and a loss in the economy. With an increase in terrorist incidents over the past decade, blast research on RC walls/slabs/panels has become increasingly important and has received significant attention by the civil engineering community. However, very limited information is available on the response of RC reservoir walls under blast loading. A thorough review of the literature on blast research on walls/slabs/panels illustrates that research on the response of reinforced concrete reservoir walls subjected to blast loading is non-existent. The experimental work presented in this paper aims to advance knowledge in this area. A limitation in this study is the absence of fluid retained behind the reservoir walls during testing. This influence requires additional testing and is beyond the scope of this paper.

2 EXPERIMENTAL PROGRAM

2.1 Details of Reservoir Walls

Within this study, two reinforced concrete walls were designed to represent typical reinforced concrete wall segments from a circular reservoir tank. They were then scaled, constructed and tested to investigate the structural response in terms of damage level due to increasing blast loading. The walls were designed following the design method prescribed in Circular Concrete Tanks without Prestressing, published by the Portland Cement Association (PCA, 1993).

The prototype reservoir tank was designed based on an assumed capacity of 10,000 m^3. The dimensions of the structure were: height of 9 m, inside diameter of 37.6 m, and thickness of 508 mm. The prototype reservoir wall section was scaled to the model size for experimental testing. The geometric scaling of 1 ⁄ 4.5 was selected to satisfy the testing limits of the shock tube, including geometry and blast loading capacity. The later was based on ensuring that the blast loading was sufficient to impose inelastic response in the test walls. Note that this scaling factor was not intended to reflect dynamic properties, but to conform to the geometry and capacity of the shock tube.

The two scaled reinforced concrete walls were identical with 100 mm thickness, 2550 mm length and 2440 mm height. Figures 1 and 2 provide the dimensions of the walls with reinforcing steel details and the wall cross section, respectively. The concrete walls were reinforced with two layers of 10M bars in the two orthogonal directions. The reinforcing bars have a nominal diameter and area of 11.3 mm and 100 mm^2, respectively. The horizontal and vertical reinforcement were spaced at approximately 130 mm and 300 mm, respectively. The concrete had an average 28-day compressive strength of 31.5 MPa, with an average strength on the day of testing of 36 MPa. The concrete slump was 120 mm. The reinforcing steel yield stress and ultimate stress were 465 MPa and 663 MPa, respectively. The concrete clear cover was approximately 11 mm to the horizontal reinforcement.

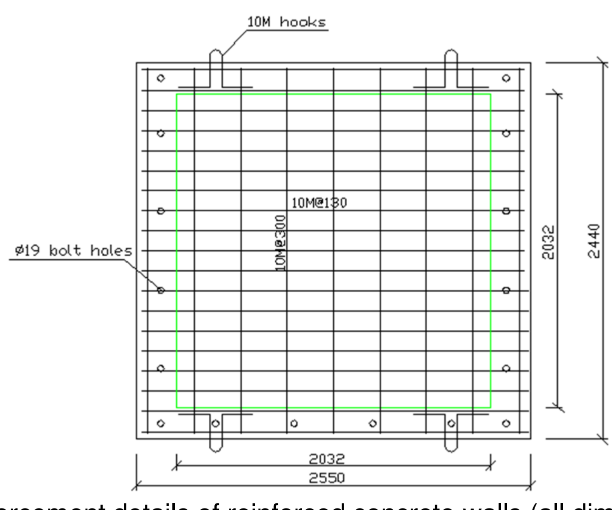

Figure 1: Reinforcement details of reinforced concrete walls (all dimensions in mm)

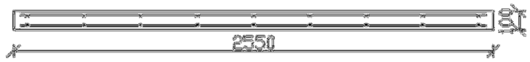

Figure 2: Cross section of reinforced concrete walls (all dimensions in mm)

The two walls were divided into two categories based on their boundary conditions: 1) two-way bending wall consisting of fixed supports on the two opposite lateral sides, and hinged base and free top edges; and 2) one-way bending wall with fixed two opposite lateral sides, and free base and top edges. The fixed lateral sides were intended to simulate the continuity of the wall, while the base support condition reflects different base supports in reservoir tanks. The free top edge represents the top of the reservoir tank. The two walls were assumed to effectively represent the behaviour of two-way and one-way walls subjected to lateral blast loading. Note that during the initial stages of the construction and instrumentation of the two walls, the intent was to test both walls with the support conditions described for Wall 1. However, after testing the first wall, it was decided to remove the base pin support for Wall 2 to investigate the response of RC reservoir tanks with a free support at the base.

The 100 mm thick two-way bending wall (Wall 1) was tested with the two opposite lateral sides fixed, the base edge hinged and the top edge free. Two, $152\ \mathrm{mm} \times 152\ \mathrm{mm} \times 6.4\ \mathrm{mm}$ hollow steel sections (HSS $152 \times 152 \times 6.4$) were used to fix the two opposite lateral sides of the wall to the shock tube testing frame. Twelve, 19 mm-diameter bolts were used to clamp together the HSS section with the wall and the test frame. In addition, four hollow steel sections with dimensions of $51\ \mathrm{mm} \times 51\ \mathrm{mm} \times 6.4\ \mathrm{mm}$ (HSS $51 \times 51 \times 6.4$) were placed horizontally and in front of the test specimen and connected to the two, $152\ \mathrm{mm} \times 152\ \mathrm{mm} \times 6.4\ \mathrm{mm}$ hollow steel sections with eight-19 mm diameter bolts. The objective was to restrain rotation of the HSS $152 \times 152 \times 6.4$ steel sections to ensure the fixed boundary condition was achieved. One-$38\ \mathrm{mm} \times 38\ \mathrm{mm} \times 4.8\ \mathrm{mm}$ angle was used on the front face of the specimen and one-$50\ \mathrm{mm} \times 50\ \mathrm{mm} \times 4.8\ \mathrm{mm}$ angle on the back face of the specimen at the base to construct a hinged support condition. Holes were drilled in the angles corresponding to the locations of bolt holes in the flange of the shock tube test frame. At the base, the wall was clamped by bolting the wall between the back-to-back angles and shock tube test frame. Details of the support conditions are illustrated in Figure 3.

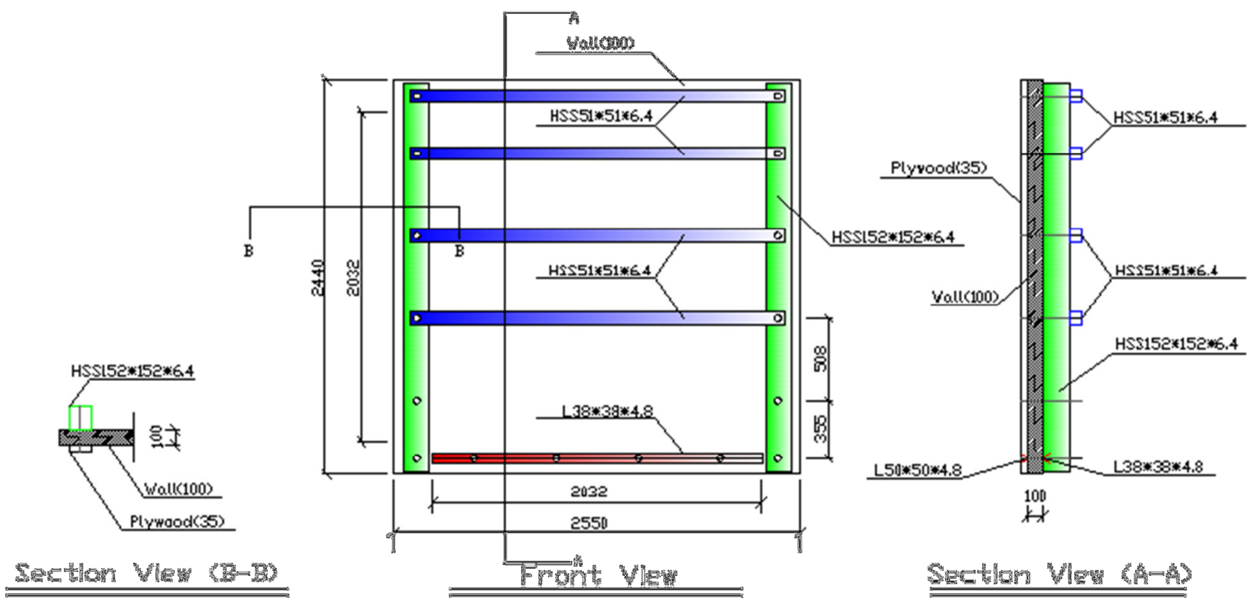

Figure 3: Boundary condition for Wall 1 (all dimensions in mm)

The 100 mm thick one-way bending wall (Wall 2) was tested with the two opposite lateral side edges fixed and free base and top edges. Two, $152\ \mathrm{mm} \times 152\ \mathrm{mm} \times 6.4\ \mathrm{mm}$ hollow steel sections (HSS $152 \times 152 \times 6.4$) were used to fix the two opposite lateral sides of the wall to the shock tube test frame with the aid of twelve-19 mm diameter bolts. In addition, six hollow steel sections (HSS $51 \times 51 \times 6.4$) were connected to the two-$152\ \mathrm{mm} \times 152\ \mathrm{mm} \times 6.4\ \mathrm{mm}$ hollow steel sections with twelve-19 mm diameter bolts to restrain the HSS $152 \times 152 \times 6.4$ from rotating. Details of the support conditions are illustrated in Figure 4.

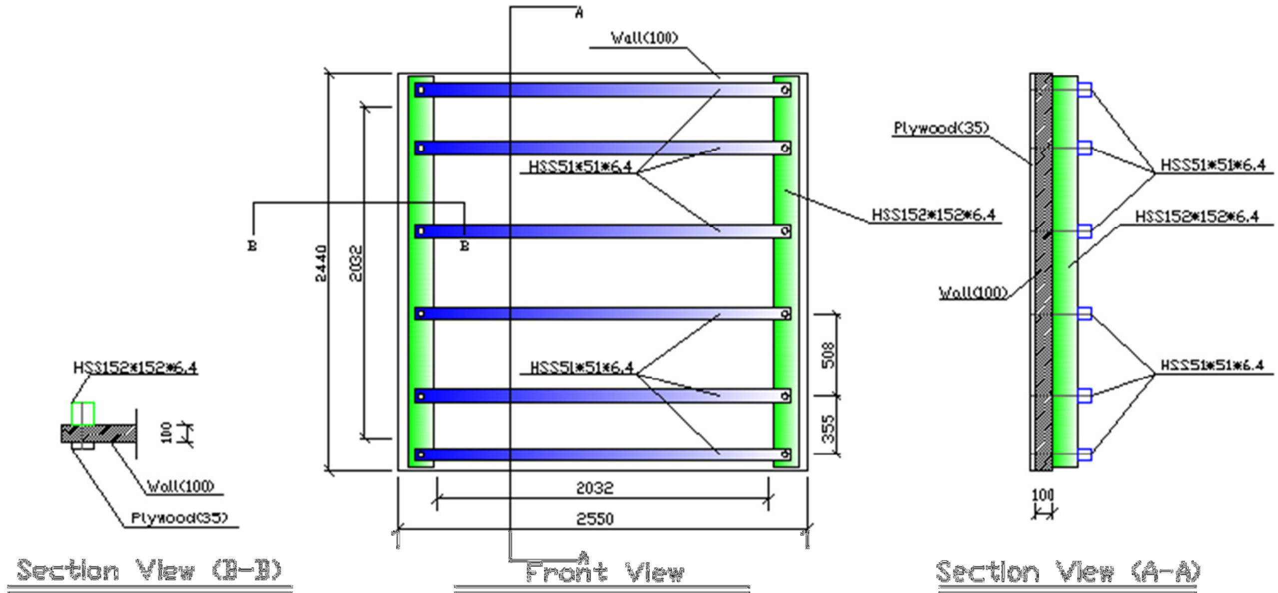

Figure 4: Boundary condition for Wall 2 (all dimensions in mm)

2.2 Test Facility and Setup

The experimental program was conducted using the shock tube testing facility in the structures laboratory at the University of Ottawa (Figure 5). The shock tube consists of four main components: (1) a variable length driver section with a double diaphragm firing mechanism; (2) a spool section used to control the firing with differential pressure; (3) an expansion section with sliding pressure relief vents; and (4) a rigid end test frame where test specimens are mounted.

Figure 5: Shock tube testing facility at University of Ottawa

2.3 Instrumentation

Each wall was instrumented with strain gauges located on selected vertical and horizontal reinforcing bars to record the strain-time histories. The location of the strain gauges was based on an assumed yield line pattern for Wall 1. Figure 6 illustrates the location of the strain gauges in the walls.

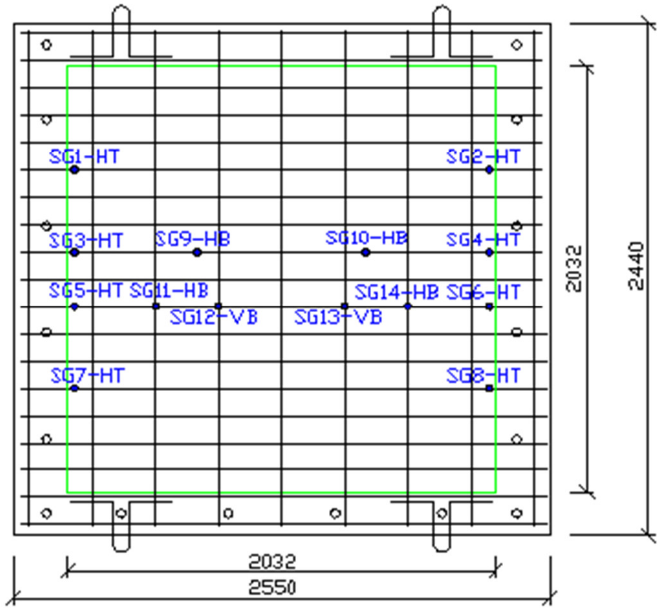

Figure 6: Location of strain gauges (all dimensions in mm)

Linear variable displacement transducers (LVDTs) were used to measure the displacements of the two walls. The LVDTs were connected where maximum displacements were expected to occur, such as at mid-span and along yield lines. In addition, LVDTs were also placed near the supports. Four LVDTs were attached to Wall 1: LVDT-Top at the maximum displacement location; LVDT-Mid at mid-span; LVDT-Rig along the assumed positive yield line; and LVDT-Lef near the left support. Also, four LVDTs were attached to Wall 2: LVDT-Mid and LVDT-Bot at the maximum displacement locations; and LVDT-Lef and LVDT-Rig at approximately half the distance from the maximum displacement location to the edges of the fixed supports.

2.4 Blast Wave Characteristics for Wall 1 and Wall 2

The two walls were exposed to blast loading that was generated through the same shock tube driver length (4880 mm). The same blast test generated different levels of damage for the different boundary conditions of Wall 1 and Wall 2. A number of the blast tests were intended to promote elastic response, while others were intended to push the walls into the inelastic range. Tables 1 and 2 provide the blast loading characteristics for each wall, including driver and reflected pressures, and reflected impulses. In addition, the values corresponding to hemispherical equivalent scaled distances, stand-off distances and TNT charge weights were established using the blast scaling law and UFC 03-340-02 (2008).

Table1: Blast wave characteristics for Wall 1

Test	Driver pressure P_d kPa	Reflected pressure P_r kPa	Reflected impulse I_r $kPa-ms$	Positive phase duration t_d ms	TNT charge weight W kg	Stand-off distance R m	Scaled distance Z $m/kg^{1/3}$
1	82.7	12.1	244.1	43.2	1064.5	208.9	20.5
2	209.6	41.9	751.1	52.2	1881.3	101.0	8.2
3	352.3	59.4	1245.2	56.6	4470.3	108.3	6.6
4	448.8	72.5	1267.6	60.4	3207.3	86.4	5.9
5	556.4	77.2	1900.1	64.6	9630.0	120.3	5.7
6	717.1	100.9	2369.2	61.4	12789.1	115.5	4.9

Table 2: Blast wave characteristics for Wall 2

Test	Driver pressure P_d kPa	Reflected pressure P_r kPa	Reflected impulse I_r $kPa-ms$	Positive phase duration t_d ms	TNT charge weight W kg	Stand-off distance R m	Scaled distance Z $m/kg^{1/3}$
1	117.2	22.4	367.8	45.4	854.8	120.5	12.7
2	212.4	41.0	670.6	57.6	1402.1	92.9	8.3
3	351.6	64.8	1102.2	52.8	2625.7	86.2	6.2
4	406.8	66.2	1304.1	57.6	4166.2	99.2	6.2
5	552.3	89.0	1794.7	59.2	6667.4	98.9	5.3
6	710.8	100.1	2122.4	54.4	9299.5	104.2	5.0

3 EXPERIMENTAL RESULTS

3.1 Summary of Test Results

This section presents the experimental results recorded from the shock tube-induced blast loading applied on the two RC reservoir walls. The results presented herein include the reflected pressure-, reflected impulse-, displacement-, and reinforcement strain-time histories. Both walls were instrumented with 10 strain gauges on the reinforcement; however, only the strains recorded from Gauges SG9-HB and SG10-HB are illustrated.

3.2 Reflected Pressures and Impulses

For Wall 1, the driver pressure was 717.1 kPa for Test 6. The resulting shock wave had a peak reflected pressure of 100.9 kPa, reflected impulse of 2369.2 $kPa - ms$ and positive phase duration of 61.4 ms. For Wall 2, the driver pressure was 710.8 kPa for Test 6. The resulting shock wave had a peak reflected pressure of 100.1 kPa, reflected impulse of 2122.4 $kPa - ms$ and positive phase duration of 54.4 ms. The reflected pressure- and impulse-time histories are presented in Figure 7.

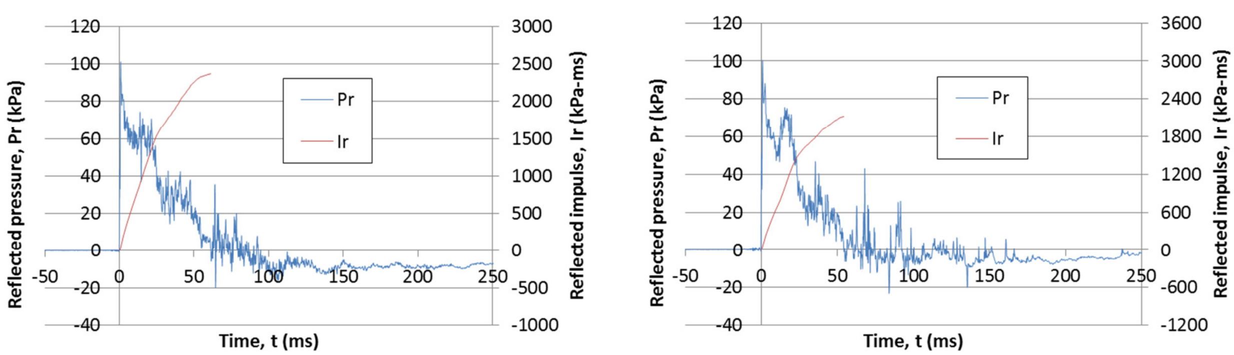

(a) (b)

Figure 7: Test 6 reflected pressure- and impulse-time histories: Wall 1; and (b) Wall 2

3.3 Displacement and Strain-time Histories

During Test 6, the maximum displacement for Wall 1 of 34.6 mm was recorded by Top LVDT, which occurred at a time of 28.2 ms. The maximum residual displacement based on Top LVDT was 3.6 mm. The displacement-time history for Wall 1 is illustrated in Figure 8 (a). The maximum displacement in Wall 2 of 33.7 mm during Test 6 was recorded by Middle LVDT, which occurred at a time of 26.6 ms. The maximum residual displacement from Bottom LVDT was 12.2 mm. The displacement-time history for Wall 2 is illustrated in Figure 8 (b).

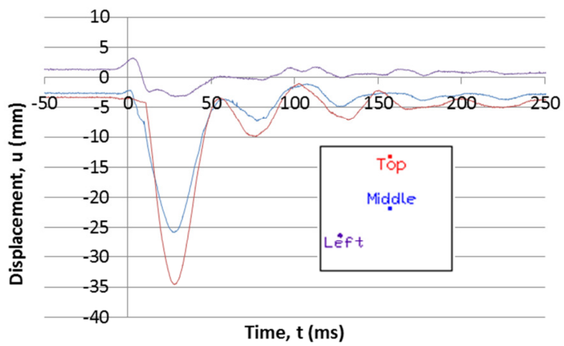

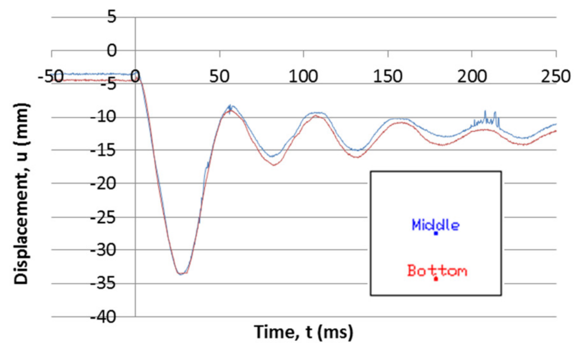

(a) (b)

Figure 8: Test 6 displacement-time histories: (a) Wall 1; and (b) Wall 2

The strain recorded by Gauge SG9-HB in Wall 1 during Test 6 was 0.25 % at a time of 25.6 ms, corresponding to a strain-rate of 0.0979 s^{-1}. The residual strain in Gauge SG9-HB was 0.059 %. The strain captured by Gauge SG10-HB was 0.38 % at a time of 27.2 ms, corresponding to a strain-rate of 0.141 s^{-1}. The residual strain in Gauge SG10-HB was 0.146 %. The strain-time histories for Gauges SG9-HB and SG10-HB for Test 6 of Wall 1 are provided in Figure 9 (a). The strain recorded by Gauge SG9-HB in Wall 2 during Test 6 was 0.15 % at a time of 26.6 ms, corresponding to a strain-rate of 0.0568 s^{-1}. The residual strain in Gauge SG9-HB was 0.0414 %. The strain captured by Gauge SG10-HB was 0.226 % at a time of 21.6 ms, corresponding to a strain-rate of 0.1046 s^{-1}. The residual strain in Gauge SG10-HB was 0.0379 %. The strain-time histories for Gauges SG9-HB and SG10-HB for Test 6 of Wall 2 are illustrated in Figure 9 (b).

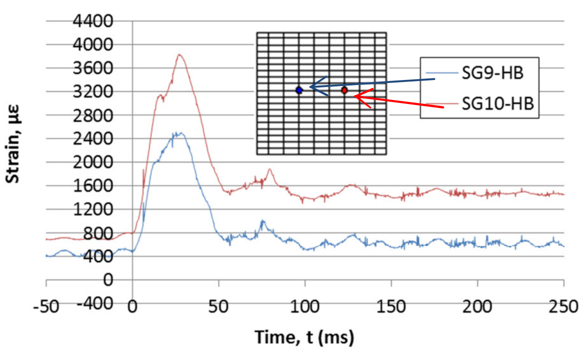

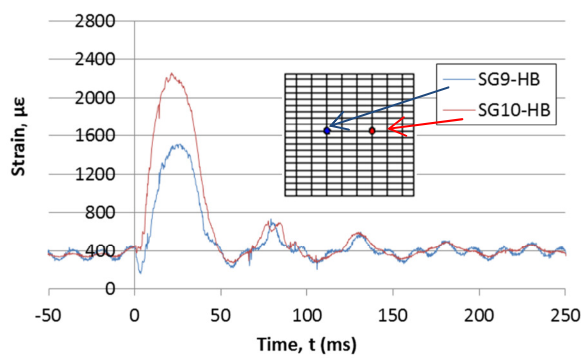

(a) (b)

Figure 9: Test 6 strain-time histories for Gauges SG9-HB and SG10-HB: (a) Wall 1; and (b) Wall 2

3.4 Cracking Patterns

For both walls, cracking continually surfaced and extended in length and width for each successive blast load. Cracking first became evident after Test 2 for both walls in the form of vertical cracking concentrated toward the middle of the wall. By the end of testing for Wall 1, the vertical cracks within the middle one-third of the wall width had the largest widths. Significant 45° inclined cracking extended from the bottom left and right corners of the wall towards the center of the wall. The cracking pattern was indicative of the yield line pattern for the support conditions of this wall. At the end of testing for Wall 2, vertical cracking near the middle of the wall extended through the entire height of the wall. Two of the vertical cracks, one located at the left and the other at the right of the one-third width of the wall, were approximately 2250 mm and 2000 mm in length, respectively. The extent of damage to the Walls 1 and 2 at the end of testing is illustrated in Figure 10.

(a)

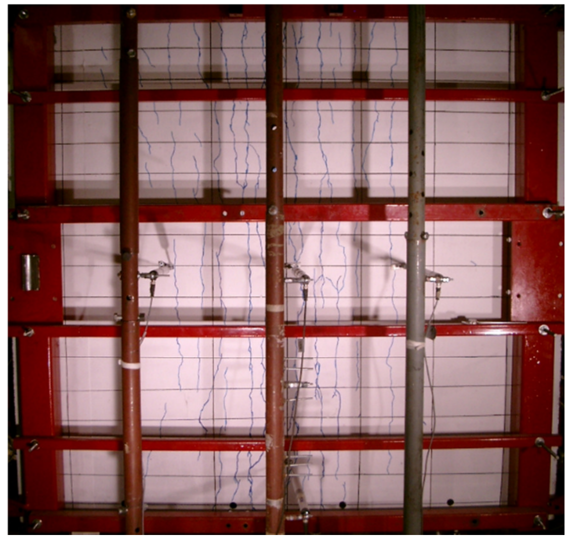

(b)

Figure 10: Condition of Walls after Test 6: (a) Wall 1; and (b) Wall 2

4 Discussion of Results

The experimental results of Wall 1 and Wall 2 are compared in this section. This includes maximum displacements recorded by the LVDTs and maximum reinforcement strains captured by the strain gauges.

4.1 Maximum Displacements

The maximum displacement in Wall 1 was 34.6 mm during Test 6, while the maximum displacement in Wall 2 was 33.7 mm during Test 6. The corresponding reflected pressures and impulses were 100.9 kPa and 2369.2 $\mathrm{kPa} - \mathrm{ms}$, and 100.1 kPa and 2122.4 $\mathrm{kPa} - \mathrm{ms}$ for Wall 1 and Wall 2, respectively. Figure 11 provides the reflected pressure-maximum displacement responses for all 6 tests for each wall. The results include readings from Top LVDT and Middle LVDT, which recorded the maximum displacements in Wall 1 and Wall 2, respectively. Furthermore, the maximum displacements recorded by the Middle LVDT for Wall 1 are included to provide a direct comparison to the Middle LVDT in Wall 2.

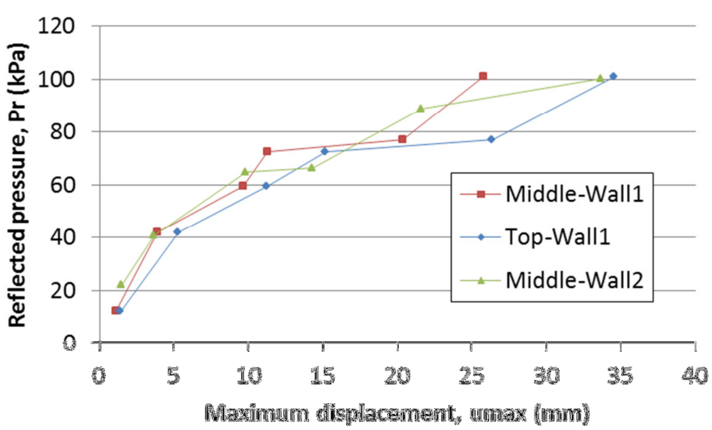

Figure 11: Reflected pressure-maximum displacement responses of Wall 1 and Wall 2

The experimental results illustrate that the displacements were, in general, slightly larger for the two-way bending wall (Wall 1) relative to the one-way wall (Wall 2) for similar blast loading beyond Test 1. This was contrary to expectations. A probable cause was the actual degree of restraint provided by the side edge supports that were intended to be fully fixed. For Wall 1, four HSS steel sections were used to span the wall and tie the edge supports, while six HSS sections were used for Wall 2. The additional horizontal tie members seem to have stiffened the edge supports, thus providing more fixity. In addition, the impulse experienced by Wall 1 was, in general, greater than Wall 2 resulting in increased displacements for Wall 1.

4.2 Maximum Reinforcement Strains

For Wall 1, the reinforcing steel yielded during Test 5 (reflected pressure of 77.2 kPa and reflected impulse of 1900.1 $\mathrm{kPa-ms}$). The maximum strain in Gauge SG10-HB was 0.26 %, which just slightly exceeded the yield strain of 0.26 % obtained from coupon tensile testing. Strains of 0.18 %, 0.17 % and 0.21 % were recorded by Gauges SG9-HB, SG11-HB and SG14-HB (see Figure 6), below the yield limit. During Test 6, the maximum strain in Gauge SG10-HB was 0.38 %, which exceeded the yield strain, while the strains recorded by SG9-HB, SG11-HB and SG14-HB were 0.25 %, just slightly below the yield limit. Recall that the location of the strain gauges was based on an assumed yield line pattern for Wall 1. As such, it appears that the gauges were properly positioned to capture yielding. For Wall 2, the strain gauges did not record strains in excess of yielding. During Test 6 (reflected pressure of 100.1 kPa and reflected impulse of 2122.4 $\mathrm{kPa-ms}$), a maximum strain of 0.23 % was captured by Gauge SG10-HB. It is probable that the strain gauges did not record yielding due to their location in the wall, which was based on an assumed yield line for Wall 1. The damage to Wall 2 was more confined at the mid-span of the specimen; however, this zone was deficient of strain gauges. Figure 12 provides the reflected pressure-maximum strain responses recorded by Gauge SG10-HB, respectively. This gauge recorded the highest strains in Walls 1 and 2.

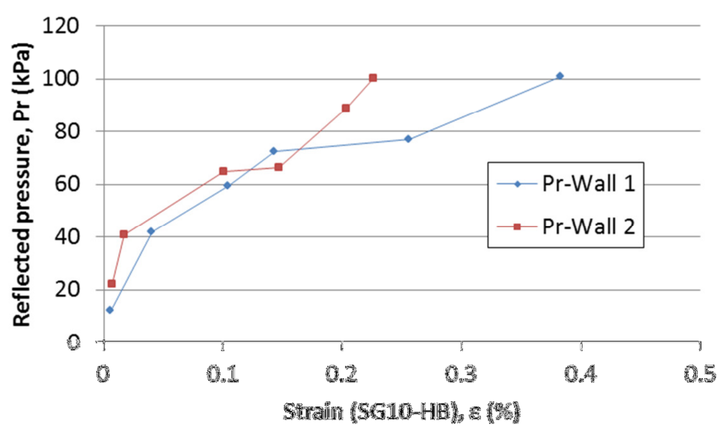

Figure 12: Reflected pressure-maximum strain responses (SG10-HB) of Wall 1 and Wall 2

4.3 Support Conditions

One of the main challenges in this experimental study was to maintain the assumed fixed side edge support conditions. The strain gauges recorded maximum tensile strains in the range of 0.025-0.05 % in the horizontal reinforcement along the side edges for Wall 1, while maximum strains of 0.015-0.04 % were recorded for Wall 2. These strains were significantly lower that the yield strain (0.26 %). In addition, simplified SDOF analyses (Fan 2014) suggested that the side supports behaved as fixed during the first few blast test. However, with increasing blast pressures, the supports began to rotate and behave more closely as pins.

5 Conclusions

The main purpose of this study was to experimentally investigate the response of RC reservoir walls subjected to blast loading. To achieve this objective, an experimental program was conducted using a shock tube that imposes loading with characteristics similar to live explosives.

Based on the experimental test results, the following conclusions can be reached:

- The reflected pressures and impulses measured during testing for the same driver length and similar drive pressures were generally in agreement for the two walls.
- The reflected impulses were positively correlated with the reflected pressures for the six blast tests for the two walls.
- During the last blast test, the maximum strain recorded by the strain gauges exceeded the yield limit in Wall 1; however, the maximum strain did not exceed the yield limit in Wall 2. The latter is attributed to the location of the strain gauges, which was based on an assumed damaged pattern for Wall 1.
- During the last blast test, both walls experiences similar maximums displacements. However, the displacements recorded in Wall1 were, in general, slight larger for most of the blast tests.
- The residual displacement in Wall 2 after the last test was significantly higher than in Wall 1. This suggests that yielding in Wall 2 did take place.

REFERENCES

Duranovic, N. 1998. Impulsive Loading on Reinforced Concrete Slabs – Modelling Considerations. *International Conference on Structures Under Shock and Impact*, SUSI, 817-826.

El-Dakhakhni, W. W., Mekky, W. F., Changiz Rezaei, S. H. 2010. Validity of SDOF Models for Analyzing Two-Way Reinforced Concrete Panels under Blast Loading. *Journal of Performance of Constructed Facilities*, 24(4): 311-325.

Fan, J. 2013. Response of Reinforced Concrete Reservoir Walls Subjected to Blast Loading. *Master of Applied Science Thesis*, University of Ottawa, Ottawa, ON, Canada.

Jacques, E. 2011. Blast Retrofit of Reinforced Concrete Walls and Slabs. *Master of Applied Science Thesis*, University of Ottawa, Ottawa, ON, Canada.

Li, Q. M. and Meng, H. 2002. Pressure-Impulse Diagram for Blast Loads Based on Dimensional Analysis and Single-Degree-of Freedom Model. *Journal of Engineering Mechanics*, 128(1): 87-92.

Lu, B., Silva, P., Nanni, A., and Baird, J. 2005. Retrofit for Blast Resistant RC Slabs With Composite Materials. *International Concrete Abstracts Portal*. American Concrete Institute (ACI). Special Publication. Vol. 230: 1345-1360.

Magnusson, J. 2007. Structural Concrete Elements Subjected to Air Blast Loading. *Licentiate thesis*, KTH, Department of Civil and Architectural Engineering, Stockholm, Sweden.

Morison, Colin M. 2006. Dynamic Response of Walls and Slabs by Single-Degree-Of-Freedom Analysis-A Critical Review and Revision. *International Journal of Impact Engineering*, 32(8): 1214-1247.

Portland Cement Association (PCA). 1993. *Circular Concrete Tanks without Prestressing*. Skokie, Illinois, USA.

Quan, X. 2005. Applications of a Coupled Multi-solver Approach in Evaluating Damage of Reinforced Concrete Walls from Shock and Impact. *18th International Conference on Structural Mechanics in Reactor Technology* (SMiRT 18), Beijing, China, 2539-2547.

Razaqpur, A. G., Tolba, A., and Contestabile, E. 2007. Blast Loading Response of Reinforced Concrete Panels with Externally Bonded GFRP Laminates. *Journal of Composites*, B38: 535-546.

Shi, Y. C., Li, Z. X., and Hao, H. 2010. A New Method for Progressive Collapse Analysis of RC Frames under Blast Loading. *Journal of Engineering Structures*, 32: 1691-1703.

Tai, Y. S., Chu, T. L., Hu, H. T., and Wu, J. Y. 2011. Dynamic Response of A Reinforced Concrete Slab Subjected to Air Blast Load. *Journal of Theoretical and Applied Fracture Mechanics*, 56(3): 140-147.

Toutlemonde, F., Rossi, P., Boulay, C., Gourraud, C., and Guedon, C. 1995. Dynamic Behaviour of Concrete: Tests of Slabs with A Shock Tube. *Journal of Materials and Structures*, 28(179): 293-298.

Unified Facilities Code (UFC) 03-340-02. 2008. *Structures to Resist the Effects of Accidental Explosions*, United States of America Department of Defense, Washington, D.C., USA.

Xu, K., and Lu, Y. 2006. Numerical Simulation Study of Spallation in Reinforced Concrete Plates Subjected to Blast Loading. *Journal of Computers & Structures*, 84(5-6): 431-438.

Zhou, X. Q., and Hao, H. 2008. Numerical Prediction of Reinforced Concrete Exterior Wall Response to Blast Loading. *Journal of Advances in Structural Engineering*, 11(4): 355-367.